Journal of Environmental Health and Sustainable Development

Impact of Gamma Radiation on Physical Characteristics of Packaging Film Made from Chitosan, Bacterial Cellulose Nanofibers, and Zinc Oxide Nanoparticles

Fariborz Pirnia [1], Jalal Sadeghizadeh Yazdi [2,3,4*], Neda Mollakhalili [2], Masoumeh Arab [2], Reyhane Sefidkar [5]

[1] *Master of Food Science and Technology, School of Public Health, Shahid Sadoughi University of Medical Sciences, Yazd, Iran.*
[2] *Department of Food Science and Technology, School of Public Health, Shahid Sadoughi University of Medical Sciences, Yazd, Iran.*
[3] *Research Center for Food Hygiene and Safety, School of Public Health, Shahid Sadoughi University of Medical Sciences, Yazd, Iran.*
[4] *Environmental Science and Technology Research Center, School of Public Health, Shahid Sadoughi University of Medical Sciences, Yazd, Iran.*
[5] *Department of Biostatistics, School of Public Health, Shahid Sadoughi University of Medical Sciences, Yazd, Iran.*

ARTICLE INFO

ORIGINAL ARTICLE

Article History:
Received: 12 November 2024
Accepted: 20 January 2025

***Corresponding Author:**
Jalal Sadeghizadeh Yazdi

Email:
j.sadeghizadeh@ssu.ac.ir

Tel:
+98 913-3584580

Keywords:
Food Packaging,
Nanocomposites,
Chitosan,
Cellulose Nanofiber,
Nanoparticles,
Gamma Rays.

ABSTRACT

Introduction: Notwithstanding the numerous benefits associated with chitosan biopolymer in the fabrication of biodegradable films, its limited mechanical properties and susceptibility to moisture represent significant barriers to its broader application within the packaging sector. Therefore, in this study, chitosan film was combined with bacterial cellulose nanofibers (BCNF) and zinc oxide nanoparticles (ZnONPs) and then exposed to different doses of gamma rays to investigate its effect on physical properties of films.

Materials and Methods: In this study, three types of films with three different formulations were prepared along with a control group, and then the effect of gamma rays on their physical characteristics in the first stage and structural properties were investigated in the second stage.

Results: The outcome showed that ZnONPs significantly decreased the water vapor permeability (WVP) and increased the opacity of films ($p < 0.05$). Differential Scanning Calorimetry (DSC) test showed that the presence of ZnONPs and gamma ray irradiation improved the heat resistance of cellulose-chitosan films. The moisture content (MC) of cellulose-chitosan films significantly decreased after being combined with zinc oxide nanoparticles and the irradiation process. The solubility of films showed a significant decrease by adding ZnONPs and increasing irradiation doses. According to the results of FTIR, the samples of the tested films under the influence of irradiation treatments did not show significant difference in the spectrogram.

Conclusion: The addition of BCNF and ZnONPs to chitosan-based films and the simultaneous application of gamma ray irradiation technology improved the physical properties of chitosan films.

Citation: Pirnia F, Sadeghizadeh Yazdi J, Mollakhalili N et al. ***Impact of Gamma Radiation on Physical Characteristics of Packaging Film Made from Chitosan, Bacterial Cellulose Nanofibers, and Zinc Oxide Nanoparticles.*** J Environ Health Sustain Dev. 2025; 10(1): 2533-50.

[DOI: 10.18502/jehsd.v10i1.18299]

Introduction

Releasing non-biodegradable plastic material waste in nature and its environmental impact is a main universal concern. Research indicates that biodegradable polymers derived from polysaccharides, proteins, and lipids are viable alternatives to conventional synthetic polymers. This assessment is primarily based on their biodegradability, biocompatibility, edibility, and the fact that they are sourced from non-petroleum materials, all of which contribute to mitigating environmental issues [1].

Chitosan($C_6H_{11}NO_4$), is a natural polysaccharide biopolymer composed of β-1,4-linked glucosamine and N-acetylglucosamine. Owing to its antimicrobial, antifungal, and antioxidant properties, chitosan is particularly suitable for the fabrication of edible films. Its advantageous characteristics include effective barrier properties against water vapor and oxygen, as well as its non-toxic nature, biodegradability, environmental compatibility, and superior film-forming capabilities. [2, 3]. Chitosan is a polymer that is easily combined with other components such as other polysaccharides, proteins, or lipids. This feature causes different properties of films to change according to the food needs that are applied to it [4]. Chitosan-based films have been effectively utilized as biopackaging materials to enhance the preservation of packaged food products [5].

Cellulose is recognized as the most prevalent biopolymer on Earth. Bacterial cellulose (BC) is a unique form of cellulose synthesized by specific bacterial species, notably *Gluconacetobacter xylinus*. Owing to its cost-effectiveness, renewability, biocompatibility, and biodegradability, BC has garnered significant attention for various applications, particularly in food packaging and biomaterials, including fibers and membranes. Notable properties of BC include its substantial water retention capacity, elevated crystallinity, mechanical strength, biological adaptability, and high purity [3, 6].

It is worth mentioning that the introduction of nanotechnology has provided new opportunities for the expansion of efficient packaging materials with excellent effects on food maintenance [7]. In recent developments, various inorganic nanoparticles, including silver, zinc, gold, and titanium, have garnered attention owing to their advantageous properties [8]. Zinc oxide nanoparticles (ZnONPs) have favorable characteristics, such as chemical stability, recyclability, high coating, antibacterial activity, and nontoxicity, which has attracted the attention of the food industry [9, 10].

The study showed that incorporating orange essential oil into (butylene adipate co-terephthalate) PBAT films at doses of 10, 25, and 50 kGy resulted in changes in the chemical structures of the films. This alteration was evident in the film differential scanning calorimetry (DSC) data, which indicated a decrease in crystallization temperature and an increase in enthalpy of fusion, suggesting cross-linking within films [11].

Researchers have concluded that applying dielectric barrier discharge (DBD) cold plasma treatment to biodegradable packaging films made from gelatin and sodium alginate, combined with silver nanoparticles, can significantly enhance their properties. This enhancement, which includes improved tensile strength, transparency, structural integrity, and barrier properties, is attributed to the addition of AgNPs and plasma treatment. Such packaging material can effectively increase the shelf life of salmon stored in a refrigerator [12].

Bakouei et al. used chitosan-based nanocomposite film containing (BCNF) and ZnONPs to increase the The investigation into the shelf life of bread revealed that the incorporation of zinc oxide nanoparticles (ZnONPs) led to an increase in the opacity of the films. Conversely, there was a significant reduction in the water vapor permeability (WVP) index. Additionally, the melting temperature (Tm) and thermal stability of the chitosan films were significantly enhanced. [13]. In another study, Salari et al. investigated the effect of using gamma radiation technology to modify a chitosan/nanocrystalline cellulose nanocomposite film, and the results showed that irradiation increased surface hydrophobicity and permeability to water vapor and improved thermal

[DOI: 10.18502/jehsd.v10i1.18299]

stability. The yellowness and opacity of the films also increased at the same time [14].

The objective of this investigation was to supply a packaging film of chitosan containing BCNF and ZnONPs and to investigate the effect of gamma radiation on its physical characteristics, including moisture, solubility, WVP, turbidity, light transmission, and thermal, spectroscopic, and structural properties.

Materials and Method

Chitosan powder (medium molecular weight, degree of deacetylation: 75-85%) and BC nanofibril gel were provided by Nano Novin Polymer Chemical Company (Iran). ZnO NPs (< 20 nm) were bought from Temad Kala Company (Iran). Other analytical grade chemicals including acetic acid (CH_3COOH), calcium sulfate ($CaSO_4$), potassium sulfate (K_2SO_4), and liquid glycerol ($C_3H_8O_3$) were acquired from Merck & Co., located in Germany.

Preparation of Nanocomposite Films

The films were fabricated using the solution casting technique. Initially, a 1% (w/v) chitosan solution was created by dissolving 1 g of chitosan powder in 100 mL of a 2% (v/v) acetic acid aqueous solution. This mixture was then subjected to sonication with a high-intensity ultrasonic processor (Ultrasonic homogenizer HD 4100, Bandelin Sonopuls, Germany) configured for intermittent pulsing with a cycle of 120s on and 15 s off, at an amplitude of 50% for 30 min (Power = 100w and Ultrasonic frequency = 20kHz). Concurrently, a suspension of BCNF was formulated at a concentration of 4% (w/w chitosan), subjected to ultrasonic treatment for 30 min, and added to the chitosan solution. In contrast, dispersions of zinc oxide nanoparticles (ZnONPs) at concentrations of 0.5%, 1%, and 2% (w/w chitosan) were prepared and subsequently incorporated into a previously formulated chitosan/bacterial cellulose nanofiber (Ch/BCNF) solution. This mixture was agitated for 30 min. Following this, glycerol, constituting 30% w/w of chitosan, was introduced as a plasticizer into the film-forming solutions, and stirring was continued for an additional 30 min. The resultant samples were then transferred into polypropylene petri dishes and subjected to drying in an oven at 25°C for 48 h. Once dried, the nanocomposite films were carefully removed from the Petri dishes and conditioned in a desiccator containing a saturated magnesium nitrate solution at 50% relative humidity (RH) for 48 h prior to further experimental evaluation [15, 16].

Irradiation of films

The Ch/BCNF and Ch/BCNF/ZnONPs films were encapsulated in polyethylene bags and subjected to gamma irradiation utilizing a gamma-cell Issledovatel (PX-30, Russia), sourced from 60 Cobalt, at the Research Institute of Radiation Application, Atomic Energy Organization of Iran. The irradiation doses administered were 5, 10, and 15 kGy, with a dose rate of 0.8 Gy/s, conducted in an air atmosphere at ambient temperature. For each treatment condition, a control batch was designated as the reference (non-irradiated).

Nanocomposite Films Characterization

Water Vapor Permeability

The water vapor permeability (WVP) of the films was assessed using the ASTM E96 standard test method, following the protocols established by Salari et al. [14]. The film samples were positioned in specialized vials, which measured 1.5 cm in diameter and 4 cm in depth, featuring an aperture of 4 mm in the lids. Each vial contained 3 g of anhydrous $CaSO_4$ to establish a relative humidity of 0%. Subsequently, the vials were weighed and placed in a desiccator maintained at 25 °C, containing a saturated solution of K_2SO_4 (RH = 97%). The relative humidity (RH) differential observed between the two sides of the films was associated with a pressure differential of 3073.93 Pa, which was interpreted as the partial pressure of water vapor. The vials were weighed every 24 h with a precision of 0.0001 g over a period of seven consecutive days. A graph depicting the changes in vial weight over time was constructed, and linear regression analysis was performed to determine the slope of the resulting line. The slope of the plot representing weight gain in relation to time (with

[DOI: 10.18502/jehsd.v10i1.18299]

an R^2 value of 0.99 or higher) was subsequently divided by the transfer area to calculate the water vapor transmission rate (WVTR). Following the determination of the WVTR, the water vapor permeability (WVP) was computed using the following equations:

$$\text{WVP (g m}^{-1}\text{ s}^{-1}\text{ Pa}^{-1}) = \frac{WVTR \times x}{\Delta P} \quad (1)$$

$$\text{WVTR(gm}^{-2}\text{s}^{-1}) = \frac{S}{A}$$

where S is the slope by linear regression, *A* is the film transfer surface, *X* is the average film thickness (*m*), and *ΔP* is the pressure difference (Pa).

Moisture content (MC)

The moisture content (MC) of the films was assessed by quantifying the weight loss of film samples (20 mm × 20 mm) prior to and following drying in a hot-air oven (Behdad Co., Iran) at a temperature of 110 ± 1°C until a constant weight was achieved [17]. The MC of the films was calculated as follows:

$$\text{MC (\%)} = \frac{Mi - Mf}{Mi} \times 100 \quad (2)$$

Mi is the initial film weight (g) and *Mf* is the dry film weight (g).

Water solubility (WS)

The water solubility (WS) of the films was investigated utilizing the methodology established by Jafarzadeh et al.[18]. The samples were prepared with standardized dimensions of 30 mm × 30 mm and subjected to conditioning in a desiccator containing silica gel for three days. Following this, the film samples were weighed and immersed in 80 mL of distilled water at 25°C for a period of 24 h, during which they were agitated at a rate of 100 revolutions per minute for one hour at ambient temperature. The residual film was subsequently filtered using filter paper and dried in an oven at 60 °C until a constant weight was achieved. The water solubility of the films was determined using the equation, where W represents the initial dry weight and W denotes the final dried weight of the film [33].

$$\text{WS (\%)} = \frac{Wi - Wf}{Wf} \times 10 \quad (3)$$

Light Transmission and Opacity

The barrier properties of the films against ultraviolet (UV) and visible light were examined at wavelengths of 200, 280, 600, and 800 nm using a UV-VIS spectrophotometer (DR6000 UV-VIS Laboratory Spectrophotometer-HACH, USA). Visible light is defined as having wavelengths ranging from approximately 380 to 740 nm, situated between the invisible infrared spectrum and shorter wavelengths of invisible UV light. Film samples measuring 40 × 10 mm were positioned directly within the test cell of the spectrophotometer, whereas an empty test cell served as the reference [18].

The opacity of the films was calculated using the following equation:

$$\text{Opacity} = \frac{Abs_{600}}{d} \quad (4)$$

Where $Abs600$ is the absorbance at 600 nm and *d* is the film thickness (mm).

Differential scanning calorimetry

The thermal characteristics of the films were examined using Differential Scanning Calorimetry (DSC) equipment (STA 6000-Perkin Elmer, USA). A sample mass of five milligrams from each film was positioned in a DSC pan, with an empty aluminum pan serving as the reference. The analysis of the samples was conducted over a temperature range of 30–260 °C, employing a heating rate of 10 °C/min in a nitrogen atmosphere at a flow rate of 20 ml/min. The nitrogen environment was employed as a neutral medium, whereas liquid nitrogen was utilized as a cooling agent [19].

Attenuated total reflectance-fourier transform infrared spectroscopy (ATR-FTIR)

The Fourier transform infrared (FT-IR) spectra of films composed of Chitosan/Bacterial Cellulose Nanofibers (Ch/BCNF) were acquired utilizing a Fourier transform infrared spectrometer equipped with an attenuated total reflectance (ATR) accessory (Thermo Avator, USA). The films were prepared in a square configuration measuring 10 mm × 10 mm and subsequently subjected to drying in an oven at a temperature of 60 °C for one night. Spectra were collected over a range of

wavenumbers from 600 to 4000 cm^{-1}, utilizing 100 scans at a resolution of 4 cm^{-1}.

Field emission scanning electron microscope (FE-SEM)

The microstructural characteristics of the surface area of the nanocomposite films were analyzed using a Field Emission Scanning Electron Microscope (FE-SEM) (TESCAN, MIRA111, Czech Republic). The films were affixed to an aluminum substrate using a silver adhesive. To enhance conductivity during imaging, the samples were coated with a thin layer of gold, approximately 5 to 6 nm in thickness, for a duration of 60 s, and an accelerating voltage of 20 kV was employed, with a magnification of 10000 ×. For each sample, a minimum of five SEM images were obtained from randomly selected areas [20].

Film thickness

The thickness of the films was assessed using a modified version of the methodology established by Barzegar et al. A digital micrometer with an accuracy of 0.001 mm was employed to measure the thickness of the fabricated films. Thickness measurements were conducted at five distinct locations on each film, and both the mean and standard deviation of the measurements were subsequently reported [21].

Statistical Analysis

Following the preparation of the films, a series of physical tests was conducted with three replications for each test. Data is summarized using mean and standard deviation metrics. The experimental design incorporated two independent variables, namely gamma irradiation doses and concentrations of ZnONPs, along with their interactions. To assess statistical differences in the properties of the various samples, analysis of variance (ANOVA) was employed using SPSS software (Version 22; SPSS Inc., Chicago, USA).

Results

Considering that in this study, three types of films (5, 10, and 15 kGy irradiated) and three different formulations (0.5, 1, and 2% of ZnONPs) were used, a control group was needed to compare the measured parameters. Therefore, gamma radiation was not used for the control samples. Three formulations with three irradiation doses resulted in nine film samples. Conversely, the interactive influence of the lack of nanoparticles with irradiation (three films) and the presence of nanoparticles without irradiation (three films) were also considered. In addition to the control film (chitosan-cellulose-without nanoparticles-without irradiation), a total of 16 films, by counting three repetitions, 48 film samples were prepared and the necessary tests were performed.

In this research, four tests were performed on all films in the first stage, including MC, solubility in water, opacity, and permeability to water vapor. Three optimal and superior films of the first stage tests (Ch-BCNF- ZnONPs 0.5% - 15KG, Ch-BCNF- ZnONPs 1% - 10KG, Ch-BCNF- ZnONPs 2% - 10KG) were selected for the second stage tests, along with seven other control films that passed the second stage tests (DSC, FTIR, FE-SEM).

Physical Properties of Films MC and Solubility in Water

Table 1 displays the moisture content (MC) and water solubility (WS) of both irradiated and non-irradiated films. The irradiated Ch/BCNF/ZnONPs films showed the lowest MC compared to chitosan/cellulose with nanoparticles and without irradiation and chitosan/cellulose without nanoparticles and with irradiation. The MC of the Ch/BCNF films decreased significantly after combining with ZnONPs and applying gamma radiation ($p < 0.05$). The lowest MC was obtained for the 10 kGy-irradiated films (with 2% and 1% ZnONPs, respectively). As indicated in Table 1, the incorporation of ZnONPs led to a notable decrease in the solubility of the Ch/BCNF films. and increasing gamma-ray doses ($p < 0.05$).

The results of two-way ANOVA related to the interaction between radiation dose and the amount of nanoparticles on the MC index (A) and WS index (B) are shown in Figure 1.

[DOI: 10.18502/jehsd.v10i1.18299]

Table 1: MC and WS of different types of non-irradiated and irradiated Ch/BCNF films

Films	MC (%)	WS (%)
Ch-BCNF	15.20 ± 0.40^{a}	21.22 ± 0.15^{a}
Ch/BCNF/ZnONPs 0.5% - 0 kGy	14.30 ± 0.23^{b}	20.50 ± 0.01^{a}
Ch/BCNF/ZnONPs 0.5% - 5 kGy	14.02 ± 0.04^{bc}	19.70 ± 0.04^{b}
Ch/BCNF/ZnONPs 0.5% - 10 kGy	13.32 ± 0.10^{c}	19.04 ± 0.11^{b}
Ch/BCNF/ZnONPs 0.5% - 15 kGy	12.20 ± 0.01^{d}	18. 80 ± 0.06^{c}
Ch/BCNF/ZnONPs 1% - 0 kGy	13.10 ± 0.06^{bc}	19.80 ± 0.06^{ba}
Ch/BCNF/ZnONPs 1% - 5 kGy	13.52 ± 0.05^{bc}	18.30 ± 0.06^{c}
Ch/BCNF/ZnONPs 1% - 10 kGy	12.40 ± 0.01^{d}	17.20 ± 0.06^{d}
Ch/BCNF/ZnONPs 1% - 15 kGy	12.89 ± 0.04^{d}	17.30 ± 0.06^{d}
Ch/BCNF/ZnONPs 2% - 0 kGy	13.80 ± 0.03^{bc}	19.30 ± 0.03^{b}
Ch/BCNF/ZnONPs 2% - 5 kGy	13.20 ± 0.05^{c}	18.10 ± 0.04^{bc}
Ch/BCNF/ZnONPs 2% - 10 kGy	11.40 ± 0.08^{e}	17.70 ± 0.05^{d}
Ch/BCNF/ZnONPs 2% - 15 kGy	12.60 ± 0.01^{d}	18.30 ± 0.06^{c}
Ch/BCNF/ZnONPs 0% - 5 kGy	14.20 ± 0.01^{b}	19.70 ± 0.08^{b}
Ch/BCNF/ZnONPs 0% - 10 kGy	13.90 ± 0.06^{b}	19.20 ± 0.06^{b}
Ch/BCNF/ZnONPs 0% - 15 kGy	14.12 ± 0.04^{b}	18.50 ± 0.03^{c}

The presence of variations within a column indicates significant differences ($P < 0.05$).
Data are means ± SD.

Water vapor permeability

Enhancing water vapor permeability (WVP) is regarded as a critical consideration in the application of nanocomposite films in food packaging [14]. Table 2 shows that the nanocomposites containing nanoparticles and irradiated showed the lowest permeability to water vapor. Therefore, the addition of ZnONPs from 0.5 to 2% and gamma irradiation from 5 to 15 kGy are effective in reducing the permeability to water vapor.

Light transmission and transparency

The properties of the films as barriers to UV-visible light were examined through the assessment of light transfer at specific wavelengths ranging from 200 to 800 nm, as detailed in Table 2. According to the obtained results, the amount of light transmission in the chitosan-cellulose nanocomposites decreased with increasing ZnO nanoparticle concentration. Gamma irradiation had an intensifying effect on this process, so that films containing nanoparticles and exposed to radiation at 10 and 15 kGy had the lowest light transmission.

The results of two-way ANOVA related to the interaction between radiation dose and the amount of nanoparticles on the WVP index (C) and opacity index (D) are shown in Figure 1.

[DOI: 10.18502/jehsd.v10i1.18299]

Table 2: WVP, light transmission percentage, and opacity of different types of non-irradiated and irradiated Ch/BCNF films

Films	Opacity (nm/mm)	Light transmission (%)				Thickness (mm)	WVP (× 10 $^{-10}$ g.m^{-1}.s^{-1}. Pa $^{-1}$)
		200 nm	280 nm	600 nm	800 nm		
Ch-BCNF	1.69 ± 0.08^{a}	0.90 ± 0.08^{a}	6.90 ± 0.14^{a}	67.27 ± 0.14^{a}	76.88 ± 0.64^{a}	0.10 ± 0^{a}	3.14 ± 0.04^{a}
Ch/BCNF/ZnONPs 0.5%- 0 kGy	1.84 ± 0.09^{b}	0.08 ± 0.08^{b}	6.63 ± 0.08^{b}	66.17 ± 0.35^{b}	75.31 ± 0.99^{b}	0.09 ± 0.01^{a}	2.20 ± 0.02^{c}
Ch/BCNF/ZnONPs 0.5%- 5 kGy	2.04 ± 0.08^{c}	0.07 ± 0.01^{c}	5.90 ± 0.14^{d}	65.05 ± 0.49^{c}	74.75 ± 0.92^{b}	0.09 ± 0.01^{a}	1.80 ± 0.06^{d}
Ch/BCNF/ZnONPs 0.5%- 10 kGy	2.34 ± 0.08^{d}	0.06 ± 0.08^{c}	5.22 ± 0.08^{e}	64.41 ± 0.28^{d}	74.13 ± 0.28^{c}	0.09 ± 0.01^{a}	1.49 ± 0.02^{d}
Ch/BCNF/ZnONPs 0.5%- 15 kGy	2.63 ± 0.03^{e}	0.07 ± 0.08^{c}	4.53 ± 0.42^{f}	63.13 ± 0.21^{e}	73.24 ± 0.78^{d}	0.08 ± 02^{a}	1.26 ± 0.04^{f}
Ch/BCNF/ZnONPs 1%- 0 kGy	2.16 ± 0.05^{c}	0.08 ± 0.08^{b}	6.05 ± 0.35^{d}	65.12 ± 0.14^{c}	74.81 ± 0.28^{b}	0.09 ± 0.01^{a}	1.92 ± 0.04^{ec}
Ch/BCNF/ZnONPs 1%- 5 kGy	2.32 ± 0.05^{d}	0.06 ± 0.08^{c}	5.52 ± 0.42^{d}	64.49 ± 0.21^{d}	74.12 ± 0.21^{c}	0.09 ± 0.01^{a}	1.57 ± 0.06^{d}
Ch/BCNF/ZnONPs 1%- 10 kGy	2.52 ± 0.04^{de}	0.06 ± 0.08^{c}	4.84 ± 0.28^{f}	63.20 ± 0.35^{e}	73.33 ± 0.78^{d}	0.09 ± 0.01^{a}	1.45 ± 0.01^{d}
Ch/BCNF/ZnONPs 1%- 15 kGy	2.84 ± 0.08^{e}	0.06 ± 0.08^{c}	4.20 ± 0.21^{g}	62.73 ± 0.57^{e}	72.59 ± 0.49^{d}	0.08 ± 02^{a}	1.23 ± 0.04^{f}
Ch/BCNF/ZnONPs 2%- 0 kGy	2.40 ± 0.03^{de}	0.07 ± 0.08^{bc}	5.67 ± 0.21^{d}	63.22 ± 0.28^{e}	72.23 ± 0.92^{e}	0.08 ± 02^{a}	1.76 ± 0.01^{de}
Ch/BCNF/ZnONPs 2%- 5 kGy	2.73 ± 0.03^{e}	0.05 ± 0.08^{d}	4.81 ± 0.28^{f}	62.94 ± 0.54^{e}	71.99 ± 0.28^{e}	0.08 ± 02^{a}	1.37 ± 0.02^{df}
Ch/BCNF/ZnONPs 2%- 10 kGy	3.10 ± 0.02^{f}	0.04 ± 0.08^{e}	4.15 ± 0.28^{g}	62.42 ± 0.21^{f}	71.54 ± 0.64^{e}	0.07 ± 02^{a}	1.13 ± 0.03^{f}
Ch/BCNF/ZnONPs 2%- 15 kGy	3.36 ± 0.03^{f}	0.05 ± 0.08^{d}	3.68 ± 0.14^{g}	61.73 ± 0.35^{f}	71.04 ± 0.21^{f}	0.07 ± 02^{a}	1.32 ± 0.04^{df}
Ch/BCNF/ZnONPs 0%- 5 kGy	1.82 ± 0.08^{b}	0.08 ± 0.08^{b}	6.63 ± 0.28^{b}	66.27 ± 0.21^{b}	75.42 ± 0.42^{a}	0.10 ± 02^{a}	3.00 ± 0.01^{a}
Ch/BCNF/ZnONPs 0%- 10 kGy	2.05 ± 0.08^{c}	0.06 ± 0.01^{c}	6.29 ± 0.21^{c}	65.34 ± 0.08^{c}	75.01 ± 0.49^{b}	0.10 ± 02^{a}	2.89 ± 0.01^{ab}
Ch/BCNF/ZnONPs 0%- 15 kGy	2.40 ± 0.02^{d}	0.07 ± 0.08^{c}	6.03 ± 0.28^{d}	65.05 ± 0.49^{c}	74.69 ± 0.14^{b}	0.09 ± 0.01^{a}	2.64 ± 0.01^{b}

Different lowercase letters within a column indicate significant differences ($P < 0.05$).

[DOI: 10.18502/jehsd.v10i1.18299]

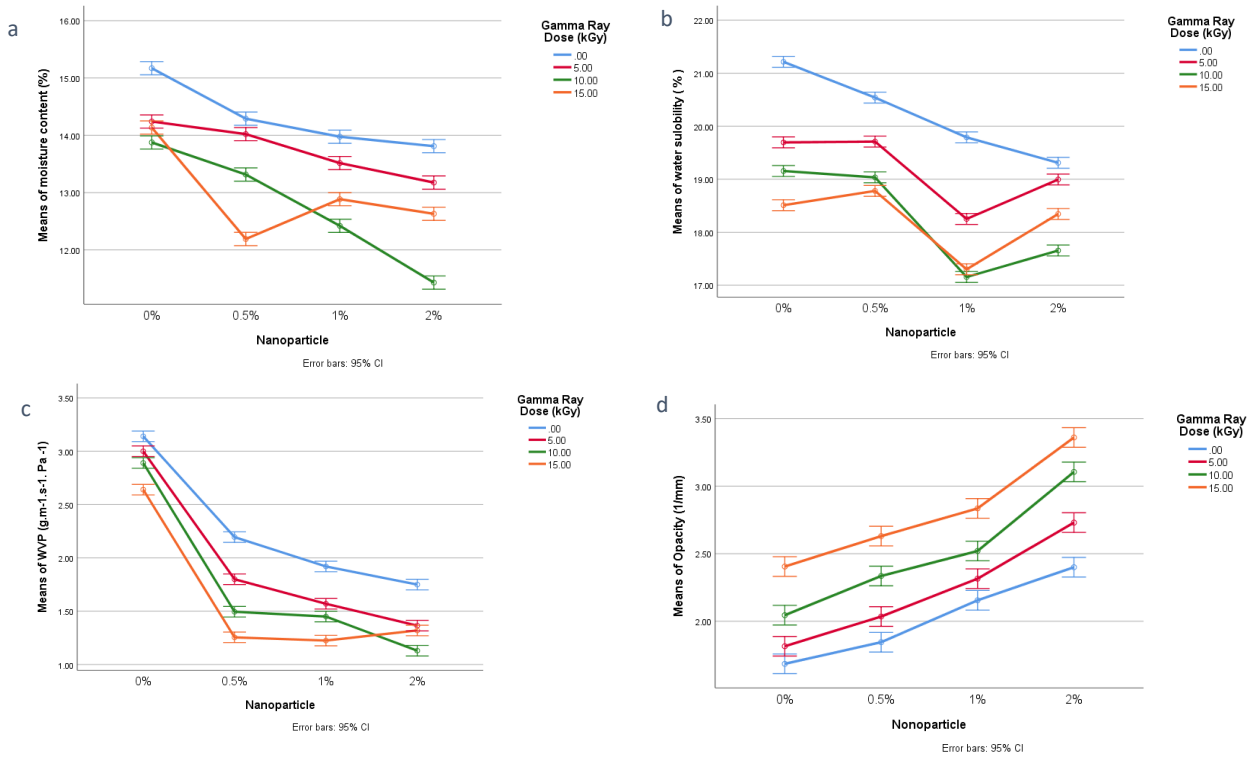

Figure 1: Two-way ANOVA diagram in investigating the simultaneous effect of radiation dose (kGy) and nanoparticle amount (%) on MC index (a) WS index (b) WVP index (c) and opacity index (d)

Thermal Properties

Thermal analysis of biopolymer nanocomposites is of great importance in the discussion of food packaging. To assess the influence of nanofibrils, nanoparticles, and gamma irradiation on the thermal characteristics of chitosan films, differential scanning calorimetry (DSC) thermograms were employed to analyze the thermal properties of the samples, that is, T_m and fusion enthalpy (ΔH_m) of the films were determined.

Figure 2 shows the DSC curves of the film samples. In these curves, the melting point was observed as an endothermic peak, which is associated with the crystalline areas of the polymer. The peak of the first endothermic reaction was taken into account as the Tm [13]. Table 3 reveals that the range of Tm for the samples was between 66-77 ° C. The addition of nanoparticles and irradiation improved the T_m values of the chitosan-cellulose films. The nanobiocomposite containing chitosan, BCNF, and 2% ZnONPs irradiated with 10 kGy gamma rays had a higher melting point (77.38 ° C), compared to the control film (68.02 ° C) and the film containing 0% of nanoparticles and 10 kGy irradiated (74.04 ° C), respectively (comparison of the interaction effect of the presence of nanoparticles).

The results of the two-way ANOVA in investigating the simultaneous effect of radiation dose and nanoparticle amount on Tm and melting enthalpy (ΔH_m) are shown in Figure 3.

[DOI: 10.18502/jehsd.v10i1.18299]

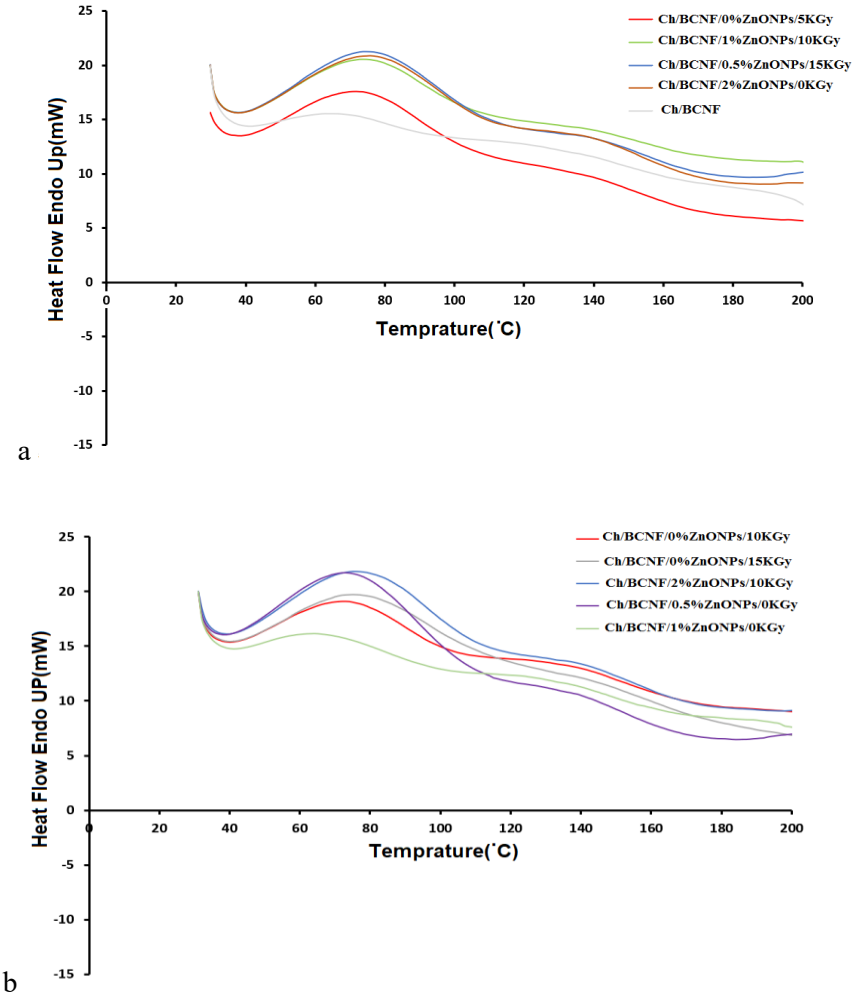

Figure 2: DSC thermograms of non-irradiated and irradiated Ch/BCNF/ZnONPs nanocomposite films

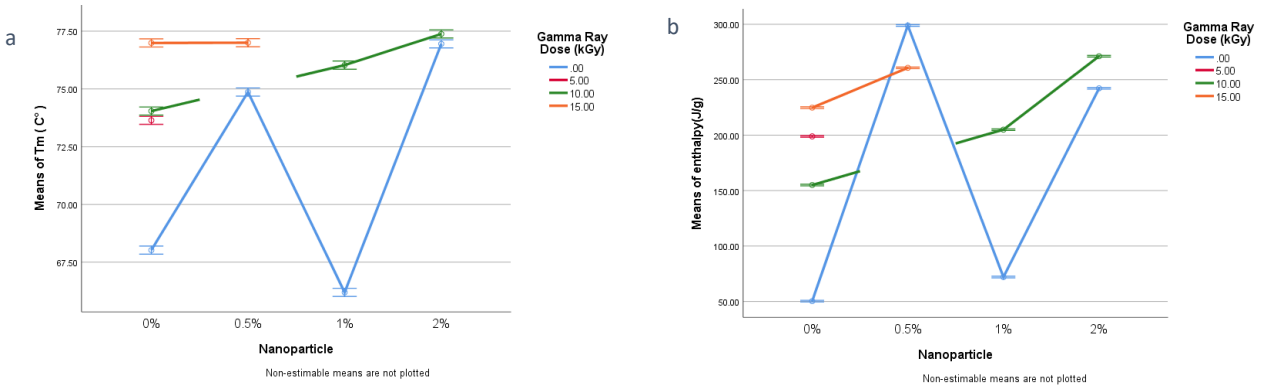

Figure 3: The results of two-way ANOVA in investigating the simultaneous effect of radiation dose and nanoparticle amount on Tm (a) and ΔH_m (b)

[DOI: 10.18502/jehsd.v10i1.18299]

Table 3: T_m and enthalpy of fusion (ΔHm) of non-irradiated and irradiated Ch/BCNF/ZnONPs nanocomposite films

Films	T_m (˚C)	ΔH_m (J/g)
Ch-BCNF	68.020 ± 0.212^{a}	50.300 ± 0.565^{a}
Ch-BCNF- ZnONPs 0% - 5KG	73.640 ± 0.070^{b}	198.895 ± 0.035^{bc}
Ch-BCNF- ZnONPs 0% - 10KG	74.040 ± 0.042^{b}	155.005 ± 0.049^{b}
Ch-BCNF- ZnONPs 0% - 15KG	76.990 ± 0.056^{c}	224.810 ± 0.183^{c}
Ch-BCNF- ZnONPs 0.5% - 0KG	74.865 ± 0.077^{b}	298.930 ± 1.046^{d}
Ch-BCNF- ZnONPs 0.5% - 15KG	77.000 ± 0.183^{c}	260.735 ± 0.770^{cd}
Ch-BCNF- ZnONPs 1% - 0KG	66.190 ± 0.098^{a}	72.015 ± 0.063^{a}
Ch-BCNF- ZnONPs 1% - 10KG	76.030 ± 0.098^{cb}	204.975 ± 0.148^{c}
Ch-BCNF- ZnONPs 2% - 0KG	76.950 ± 0.084^{cb}	242.230 ± 0.169^{c}
Ch-BCNF- ZnONPs 2% - 10KG	77.380 ± 0.056^{c}	271.200 ± 0.014^{dc}

Distinct lowercase letters within a column signify statistically significant differences ($P < 0.05$).
Data are means ± SD.

Fourier spectroscopy

The ATR-FTIR spectra for the non-irradiated chitosan/cellulose nanofiber (Ch/BCNF) films, as well as for the Ch/BCNF films incorporated with zinc oxide nanoparticles (ZnONPs) and subjected to gamma radiation doses of 5, 10, and 15 kGy, are shown in Figure 4. The data indicates that the absorption peaks observed in the spectra of the pure and non-irradiated chitosan-cellulose films closely resemble those of the irradiated Ch/BCNF films. Notably, no significant variations were observed in the spectrograms, suggesting that the chemical structure remained largely unchanged following exposure to these doses of gamma radiation (5, 10, and 15 kGy).

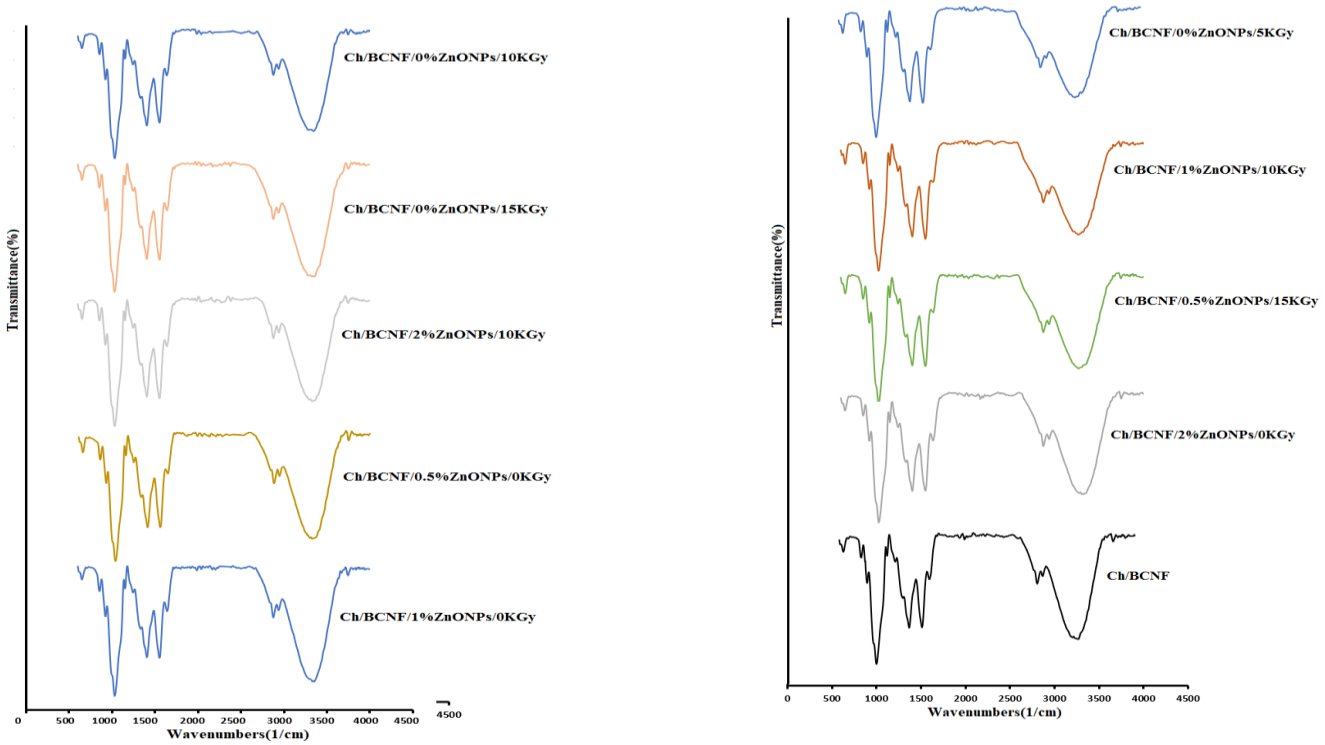

Figure 4: ATR-FTIR spectra of different types of non-irradiated and irradiated Ch/BCNF films (in color).

[DOI: 10.18502/jehsd.v10i1.18299]

Microstructure and Morphological properties

To better understand the physicochemical properties of the film samples, microstructural analysis can be useful. To this end, the film homogeneity, the presence of ZnONPs on the surface of nanocomposite layers, and the possible effects of gamma radiation and ionizing rays were investigated using a scanning electron microscope (FE-SEM).

The results of the morphological observation of the surfaces of the films containing nanoparticles, the irradiated films, and the control sample are shown in **Figure 5**. Scanning electron microscopy showed a relatively smooth and uniform coating of the control film (chitosan-cellulose). In other words, BC nanofibers were uniformly and homogeneously spread in the chitosan polymer matrix (Image No. 1 of Figure 5).

By adding ZnONPs, aggregation and agglomeration were observed in some of the points. Nanoparticle treatment made the film surfaces rougher and more uneven. However, it showed a good dispersion of nanoparticles in the nanocomposite matrix and confirmed the proper compatibility of ZnONPs with chitosan-cellulose films.

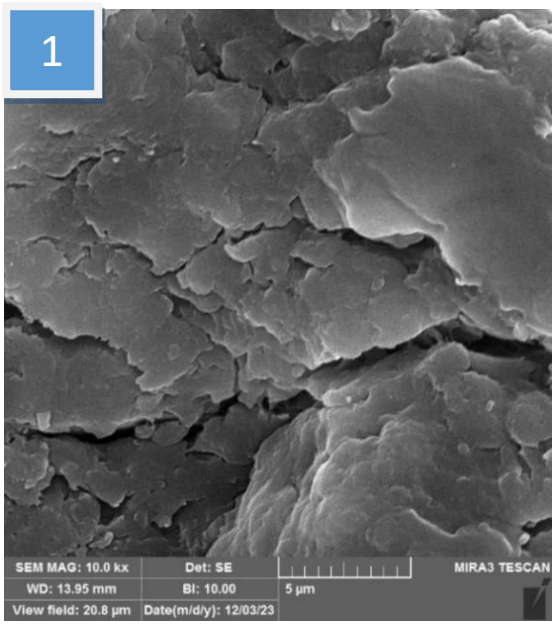

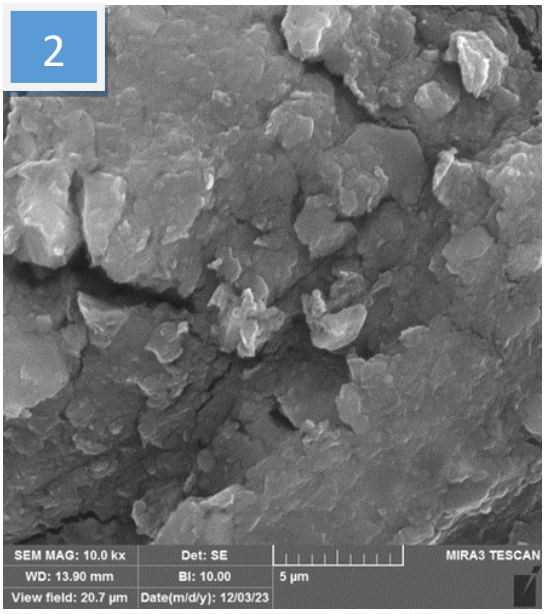

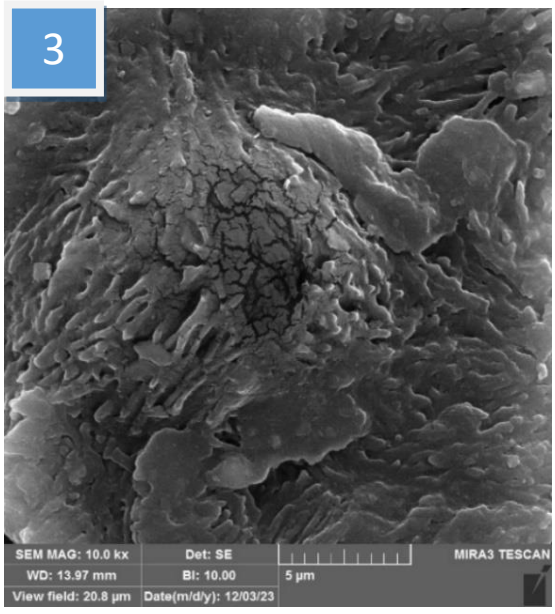

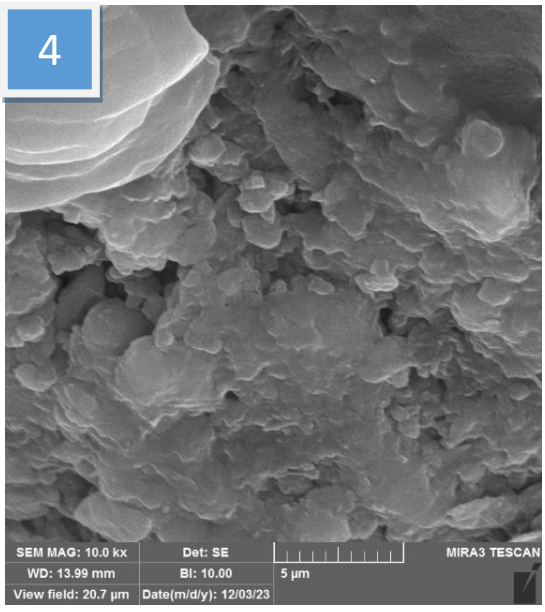

[DOI: 10.18502/jehsd.v10i1.18299]

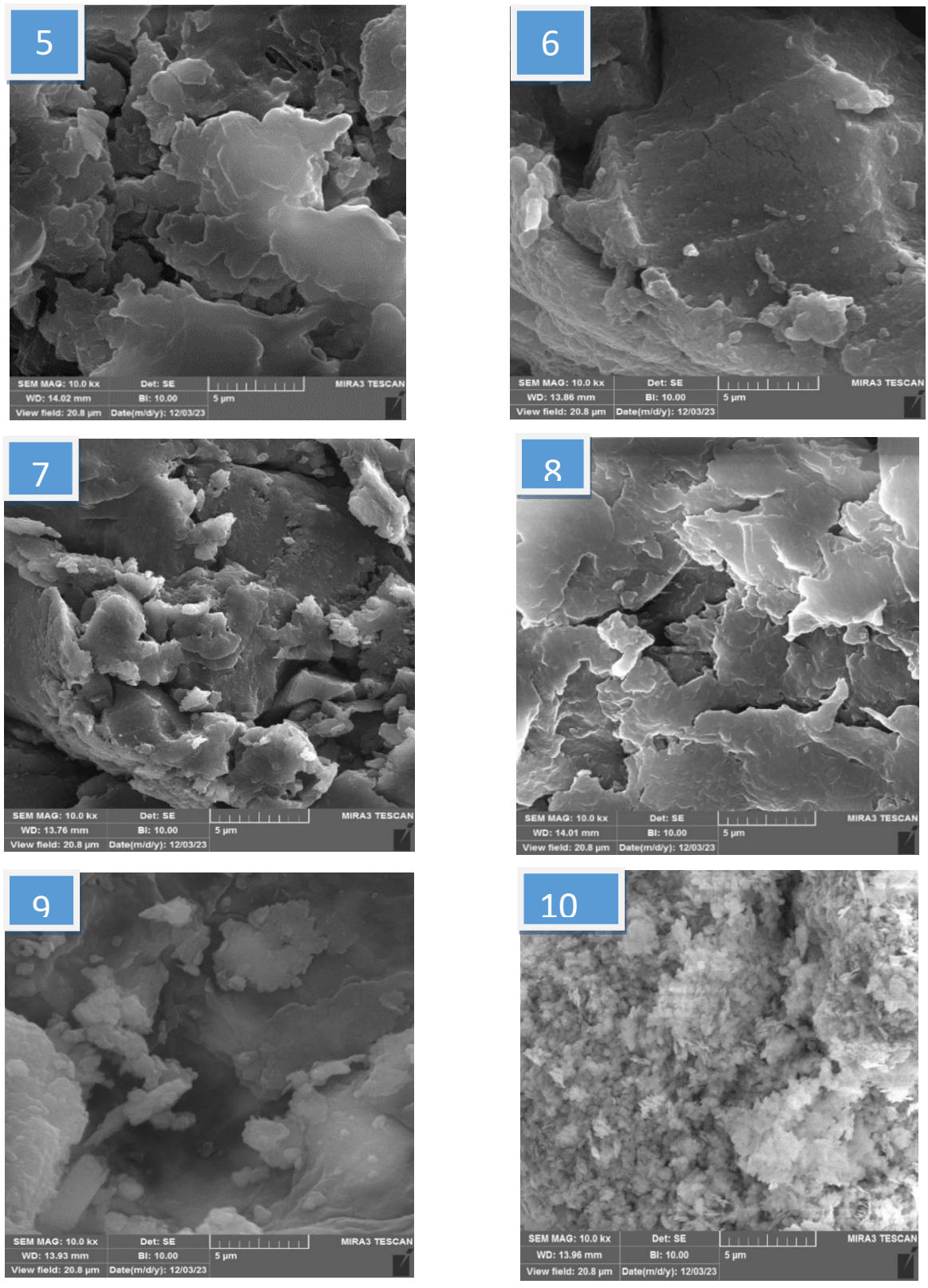

Figure 5: Images of the surface taken at a microscopic level of different types of Ch/BCNF films irradiated with 0, 5, 10, 15 KGy and containing 0, 0.5, 1, 2% ZnONPs: 1- Ch-BCNF (non-irradiated and without ZnONPs). 2- Ch-BCNF-ZnONPs 0% -5KGy. 3- Ch-BCNF-ZnONPs 0% -10KGy. 4- Ch-BCNF-ZnONPs 0% -15KGy. 5- Ch-BCNF-ZnONPs 0.5% -0KGy. 6- Ch-BCNF-ZnONPs 0.5% -15KGy. 7- Ch-BCNF-ZnONPs 1% -0KGy. 8- Ch-BCNF-ZnONPs 1% -10KGy. 9- Ch-BCNF-ZnONPs 2% -0KGy. 10- Ch-BCNF-ZnONPs 2% -10KGy.

[DOI: 10.18502/jehsd.v10i1.18299]

Discussion

These findings indicate that the moisture content (MC) values of all films diminished with the incorporation of zinc oxide nanoparticles (ZnONPs) into chitosan-cellulose-based films. This reduction in moisture content can be attributed to the enhanced compactness of the film network resulting from the addition of nanoparticles [22]. Furthermore, a significant decrease in the MC of the chitosan/bacterial cellulose nanofiber (Ch/BCNF) films was observed following irradiation. This decrease is likely due to the enhanced hydrophobic characteristics of the polysaccharide-based polymer matrix that occur as a result of gamma irradiation [23].

Solubility is one of the essential parameters of edible films as a protective coating of food. The lowest solubility in water was assigned to the 10 kGy-irradiated film with 1% ZnO NPs (17.20%). This phenomenon may be attributed to the formation of hydrogen bonds between the hydrophilic groups of chitosan and the hydroxyl groups on the surface of cellulosic nanofibrils, as well as the oxygen atom of nano zinc oxide, which improves biopolymer matrix cohesion and reduces water sensitivity [16]. Sabaghi et al. stated that a dose of 60 kGy of gamma rays significantly ($p < 0.05$) reduced the WS of films owing to the creation of a denser structure than that of the control sample [17]. In another study, Shahabi-Ghahfarrokhi et al. also stated that the WS of films in kefir-cellulose nanocomposites decreased by adding ZnONPs, which is consistent with the present study [24].

WVP. The results of this study confirmed that ZnONPs significantly reduced WVP ($p < 0.05$). On the other hand, the permeability of nanocomposite films decreased by applying radiation treatment (increasing radiation doses). The beneficial impact of irradiation on the permeability of chitosan-based films has been documented by other researchers as well [14, 23, 25]. The observed decrease in water vapor permeability (WVP) could be due to the production of free radicals as a result of exposure to radiation, which facilitates cross-linking among polymer chains, resulting in a denser and more cohesive structural configuration [14]. The WVP of Ch/BCNF films decreased after the incorporation of ZnONPs. This is associated with the reduction of free hydrophilic groups (OH) caused by the establishment of hydrogen bonds between the biopolymer matrix and ZnONPs, an increase in biopolymer crystallinity, the creation of complex pathways for water molecules, and a further rise in biopolymer crystallinity [15, 26, 27]. Bakouei et al. confirmed the improvement of permeability to water vapor as a result of adding ZnONPs to nanocomposite films [13].

Light transmission and transparency. The results showed that composite films combined with ZnONPs had less transparency and showed excellent barrier properties against the passage of UV light. The opacity of the chitosan-cellulose films increased with increasing irradiation dose and ZnO concentration ($p < 0.05$). It should be noted that the thickness of the prepared films was also reduced by adding ZnONPs and applying radiation treatment (from 0.10 to 0.07 mm).

The enhancement of film opacity through the incorporation of zinc oxide nanoparticles (ZnONPs) can be attributed to the inherent characteristics of ZnONPs as an inorganic material that remains insoluble within the polymer matrix. This effect is associated with the ability of nanoparticles to augment the light barrier properties of chitosan-based films by facilitating light scattering and obstructing light transmission, particularly when nanoparticles are uniformly integrated into the polymer matrix [13]. Gamma irradiation also made the color of the films yellower and darker to some extent, reduced the amount of light transfer, and increased the opacity of films.

The obtained outcomes were consistent with the findings produced by Noshirvani et al.[15], Bakouei et al.[13], Akter et al.[28], and Pantani et al.[29] regarding the effect of ZnONPs on the opacity of nanocomposite films and also Paula et al. [30], Salari et al. [14], Abd El-Rahim et al.[25], Zainol et al.[31], Jipa et al.[32], and Shahabi-Ghahfarrokhi et al.[24] The effects of applying gamma irradiation on improving the rate of light transmission and the opacity characteristics of composite films were

[DOI: 10.18502/jehsd.v10i1.18299]

remarkable.

Thermal Properties. As mentioned in the results, there was an increase in Tm by adding nanoparticles, which can be explained by the fact that the presence of nanoparticles enhances the overall crystallinity of the biopolymer and creates compact, dense, and regular crystals (larger crystals exhibit enhanced thermodynamic stability), finally leading to the improvement and promotion of thermal characteristics [16]. Tm is related to the characteristics of the crystalline regions of the polymer. As a result of the compression of the chains, nanoparticles typically encounter difficulties in penetrating the crystalline regions. However, they can influence the enhancement of order and facilitate the transition of amorphous regions into crystalline structures [33].

The enthalpy of melting (ΔHm) of the films is influenced by their structural configuration. The ΔHm of chitosan films increased with the integration of nanoparticles into the chitosan polymer framework. This suggests that the nanoparticles facilitated the encapsulation of chitosan chains and promoted additional cross-linking among them. These findings indicate that nanoparticles, by functioning as additives that improve the interactions among polymer chains, can enhance the thermal properties of polymers [34, 35].

Bakouei et al. showed that adding ZnONPs at three levels (0.5, 1, and 2%) to chitosan-based nanocomposite films to cover the surface of bulk bread increases the T_m values and thermal stability of chitosan-based films [13]. Studies conducted by Pantani et al. and Asadi and Pirsa et al. The findings concerning the influence of zinc oxide nanoparticles (ZnONPs) and titanium dioxide on enhancing the thermal stability of the nanocomposite film align with the results of the current investigation [29, 36].

The outcomes of this study demonstrated that the thermal properties of film samples were enhanced through the application of gamma irradiation manipulation. The T_m values increased by incorporating nanoparticles into the film matrix, and in this regard, the irradiated films containing nanoparticles showed optimal values. The increase in Tm and ΔH_m caused by irradiation can be attributed to the fact that low doses of gamma rays increase the crosslinks between biopolymer chains [14]. On the other hand, the influence of gamma irradiation on the thermal properties of biopolymers seems to be associated with the type of polymer and the amount of radiation received. Shahabi Ghahfarrokhi et al. reported that T_m of kefir-based nanocomposite films remained constant despite variations in the gamma irradiation dose [25]. In another study, the melting point of polyvinyl amide/chitosan composites increased after 50 kGy irradiation with gamma rays, whereas irradiation with higher amounts (100 and 200 kGy) decreased the melting point [37].

Salari et al. showed that the use of irradiation technology and the use of gamma rays improved the thermal steadiness of films made from chitosan and increased the T_m of both chitosan and chitosan/cellulose nanocrystal films [14].

T_m and ΔH_m of the film samples increased by adding ZnONPs, irradiation, or both, which confirms that irradiation and the presence of nanoparticles can improve the thermal stability of the chitosan-based film (Figure 3).

ATR-FTIR. Based on previous research and the principles of infrared spectroscopy, it has been determined that the existence of a broad spectrum from 3100 to 3600 cm^{-1} shows the essential vibrational modes of hydroxyl groups (O-H) due to water and carbohydrates. The spectrum from 2800 to 3000 cm^{-1} is related to the symmetric and anti-symmetric stretching modes of C-H in methyl (CH_3) and methylene (CH_2) functional groups, 1580–1700 cm^{-1} is assigned to the bending mode of O-H in water molecules, and 900–1200 cm^{-1}a is a broad and strong band associated with the stretching vibrations of carbohydrate rings and their side groups (C-O C, C-OH, C-H). The absorption peak at 1050 cm^{-1} was due to C–O stretching, and the absorption band around 2941 cm^{-1} was related to the amino group. Distinctive absorption peaks of cellulose nanofibrils appear at 3230–3455 cm^{-1} (OH stretching), 1463 cm^{-1} (CH_2 bending), and 1063-1161 cm^{-1} (saccharide

[DOI: 10.18502/jehsd.v10i1.18299]

structure) [14, 38].

Paula et al. used FTIR spectroscopy to evaluate the effects of gamma radiation on poly-caprolactone-ZnONPs and pure poly-caprolactone nanocomposite films. The results before and after gamma irradiation with a dose of 25 kGy showed a similar spectrum for both films without changing the position of the peaks [32]. Salari et al. also stated that during gamma irradiation in order to modify chitosan nanocomposite films/ BC nanocrystals, no significant changes or differences happened in the chemical functional groups of the films during irradiation and doses used (5, 10 and 15 kGy) did not cause significant changes in the infrared spectrum of films [14].

The outcomes are according to the results of Zainol et al. , Elsawy et al. ,Liu et al., and Augustine et al.[9, 31, 39, 40]. These findings show that the chemical structure of the nanocomposite films containing BC nanofibers and ZnONPs was resistant to the attacks of 5, 10, and 15 kGy gamma rays.

Microstructure and Morphological properties. The findings obtained in the research of Bakouei et al., Paula et al., and Shahabi-Ghahfarrokhi et al. regarding the positive effects of ZnONPs in improving the morphological characteristics of nanocomposite films are consistent with the present study [13, 25, 32]. However, as a result of the gamma-ray irradiation treatment, the exterior of the films gradually became smoother and more uniform, which was in good agreement with the results of the study by Salari et al.[14]. In general, the optimized films treated with gamma rays showed compact surface structures with better structural integrity, which was not observed in the untreated samples.

Conclusion

In this study, a chitosan packaging film containing BC nanofibers and ZnONPs was prepared and the effect of gamma rays on their physical properties was investigated. According to the results, the chitosan film containing BCNF, 2% ZnONPs, and 10 kGy irradiation was chosen as the optimal film by showing the best physical characteristics. Moreover, the addition of ZnONPs and the irradiation of films with gamma rays led to an increase in the thermal stability of the chitosan-cellulose films. By adding ZnONPs and increasing the doses of gamma rays, the amount of opacity increased, and transparency and permeability to water vapor decreased, which indicated the improvement of the physical properties of the films after receiving the above treatments. The MC and solubility of the chitosan/cellulose films decreased significantly by adding ZnONPs and increasing the irradiation doses. The FTIR test results did not show a significant difference between the irradiated and non-irradiated films. The results of examining the morphology of the films showed the homogeneous and appropriate diffusion of nanoparticles in films, and it was found that with the enhancement in the accumulation of nanoparticles and the absorption of gamma rays, the structure of the films became more compact and denser. Based on this evidence, this type of packaging film is suggested for use on food surfaces.

Acknowledgments

The authors gratefully thank the deputy of research and technology of Shahid Sadoughi University of Medical Sciences for their financial support. The researchers did not receive any specific grants from funding agencies in the commercial or non-profit sectors.

Conflicts of Interest

The authors declare no conflicts of interest.

Funding

This research was financially supported by the Shahid Sadoughi University of Medical Sciences. The results of this study were drawn from the MSc thesis (grant number: 14955), registered at Shahid Sadoughi University of Medical Sciences.

Ethical Considerations: Given that only the physicochemical properties of the films were evaluated in this study,

Code of Ethics: IR.SSU.SPH.REC.1401.216

Data Availability

The data used to support the findings of this study are available from the corresponding author

[DOI: 10.18502/jehsd.v10i1.18299]

upon request.

Authors contribution

J.S.Y., N.M., M.A. designed and edited the study; F.P. conducted the experimental work; R.S analyzed the data; all authors discussed the results and contributed to the final manuscript.

References

1. Sarwar MS, Niazi MBK, Jahan Z, et al. Preparation and characterization of PVA/nanocellulose/Ag nanocomposite films for antimicrobial food packaging. Carbohydr Polym. 2018;184:453-64.
2. Elsabee MZ, Abdou ES. Chitosan based edible films and coatings: a review. Materials science and engineering: C. 2013;33(4):1819-41.
3. Khan A, Khan RA, Salmieri S, et al. Mechanical and barrier properties of nanocrystalline cellulose reinforced chitosan based nanocomposite films. Carbohydr Polym. 2012;90(4):1601-8.
4. Cazón P, Vázquez M. Mechanical and barrier properties of chitosan combined with other components as food packaging film. Environ Chem Lett. 2020;18(2):257-67.
5. No H, Meyers SP, Prinyawiwatkul W, et al. Applications of chitosan for improvement of quality and shelf life of foods: a review. J Food Sci. 2007;72(5):R87-100.
6. Ashori A, Sheykhnazari S, Tabarsa T, et al. Bacterial cellulose/silica nanocomposites: preparation and characterization. Carbohydr Polym. 2012;90(1):413-8.
7. Enescu D, Cerqueira MA, Fucinos P, et al. Recent advances and challenges on applications of nanotechnology in food packaging. a literature review. Food and Chemical Toxicology. 2019;134:110814.
8. Kanmani P, Rhim J-W. Physical, mechanical and antimicrobial properties of gelatin based active nanocomposite films containing AgNPs and nanoclay. Food Hydrocoll. 2014;35:644-52.
9. Liu J, Hu J, Liu M, et al. Migration and characterization of nano-zinc oxide from polypropylene food containers. Am J Food Technol. 2016;11:159-64.
10. Pirsa S, Shamusi T, Kia EM. Smart films based on bacterial cellulose nanofibers modified by conductive polypyrrole and zinc oxide nanoparticles. J Appl Polym Sci. 2018;135(34):46617.
11. de Andrade MF, Caetano VF, de Lima Silva ID, et al. Influence of different gamma radiation doses on the physical, chemical and thermal properties of antimicrobial active packaging of poly (butylene adipate co-terephthalate)(PBAT) films additivated with orange essential oil. Polym Bull (Berl). 2024;81(7):6349-62.
12. Tahmouzi S, Sadeghizadeh-Yazdi J, Mohajeri FA, et al. The effect of the DBD cold plasma process on the physicochemical, mechanical, and microbial properties of the biodegradable packaging film (based on gelatin-sodium alginate) incorporated with AgNPs to extend the shelf life of trout fish in the refrigerator. Food Bioproc Tech. 2025;18(1):701-24.
13. Bakouei M, Sadeghizadeh Yazdi J, Ehrampoush MH, et al. The effect of active chitosan films containing bacterial cellulose nanofiber and ZnO nanoparticles on the shelf life of loaf bread. J Food Qual. 2023;2023(1):7470296.
14. Salari M, Khiabani MS, Mokarram RR, et al. Use of gamma irradiation technology for modification of bacterial cellulose nanocrystals/chitosan nanocomposite film. Carbohydr Polym. 2021;253:117144.
15. Noshirvani N, Ghanbarzadeh B, Mokarram RR, et al. Novel active packaging based on carboxymethyl cellulose-chitosan-ZnO NPs nanocomposite for increasing the shelf life of bread. Food Packag Shelf Life. 2017;11:106-14.
16. Salari M, Khiabani MS, Mokarram RR, et al. Development and evaluation of chitosan based active nanocomposite films containing bacterial

[DOI: 10.18502/jehsd.v10i1.18299]

cellulose nanocrystals and silver nanoparticles. Food Hydrocoll. 2018;84:414-23.
17. Sabaghi M, Maghsoudlou Y, Kashiri M, et al. Evaluation of release mechanism of catechin from chitosan-polyvinyl alcohol film by exposure to gamma irradiation. Carbohydr Polym. 2020;230:115589.
18. Sahraee S, Milani JM, Ghanbarzadeh B, et al. Physicochemical and antifungal properties of bio-nanocomposite film based on gelatin-chitin nanoparticles. Int J Biol Macromol. 2017;97:373-81.
19. Peng Y, Wu Y, Li Y. Development of tea extracts and chitosan composite films for active packaging materials. Int J Biol Macromol. 2013;59:282-9.
20. Dai H, Ou S, Huang Y, et al. Utilization of pineapple peel for production of nanocellulose and film application. Cellulose. 2018;25:1743-56.
21. Barzegar H, Azizi MH, Barzegar M, et al. Effect of potassium sorbate on antimicrobial and physical properties of starch–clay nanocomposite films. Carbohydr Polym. 2014;110:26-31.
22. Ojagh SM, Rezaei M, Razavi SH, et al. Development and evaluation of a novel biodegradable film made from chitosan and cinnamon essential oil with low affinity toward water. Food Chemistry. 2010;122(1):161-6.
23. Kim JK, Jo C, Park HJ, et al. Effect of gamma irradiation on the physicochemical properties of a starch-based film. Food Hydrocoll. 2008;22(2):248-54.
24. Shahabi-Ghahfarrokhi I, Khodaiyan F, Mousavi M, et al. Preparation of UV-protective kefiran/nano-ZnO nanocomposites: physical and mechanical properties. Int J Biol Macromol. 2015;72:41-6.
25. Abd El-Rehim H, Kamal H, Hegazy E-SA, et al. Use of gamma rays to improve the mechanical and barrier properties of biodegradable cellulose acetate nanocomposite films. Radiation Physics and Chemistry. 2018;153:180-7.
26. Nafchi AM, Mahmud S, Robal M. Antimicrobial, rheological, and physicochemical properties of sago starch films filled with nanorod-rich zinc oxide. J Food Eng. 2012;113(4):511-9.
27. Yu J, Yang J, Liu B, et al. Preparation and characterization of glycerol plasticized-pea starch/ZnO–carboxymethylcellulose sodium nanocomposites. Bioresour Technol. 2009; 100(11):2832-41.
28. Akter N, Khan RA, Salmieri S, et al. Fabrication and mechanical characterization of biodegradable and synthetic polymeric films: effect of gamma radiation. Radiation Physics and Chemistry. 2012;81(8):995-8.
29. Pantani R, Gorrasi G, Vigliotta G, et al. PLA-ZnO nanocomposite films: water vapor barrier properties and specific end-use characteristics. Eur Polym J. 2013;49(11):3471-82.
30. Paula M, Diego I, Dionisio R, et al. Gamma irradiation effects on polycaprolactone/zinc oxide nanocomposite films. Polímeros. 2019;29(1):e2019014.
31. Zainol I, Akil HM, Mastor A. Effect of γ-irradiation on the physical and mechanical properties of chitosan powder. Materials Science and Engineering: C. 2009;29(1):292-7.
32. Jipa IM, Stroescu M, Stoica-Guzun A, et al. Effect of gamma irradiation on biopolymer composite films of poly (vinyl alcohol) and bacterial cellulose. Nucl Instrum Methods Phys Res B. 2012;278:82-7.
33. Frone AN, Berlioz S, Chailan J-F, et al. Morphology and thermal properties of PLA–cellulose nanofibers composites. Carbohydr Polym. 2013;91(1):377-84.
34. Nasreen Z, Khan MA, Mustafa A. Improved biodegradable radiation cured polymeric film prepared from Chitosan-Gelatin blend. Journal of Applied Chemistry. 2016;2016(1):5373670.
35. Shankar S, Reddy JP, Rhim J-W, et al. Preparation, characterization, and antimicrobial activity of chitin nanofibrils reinforced carrageenan nanocomposite films. Carbohydr Polym. 2015;117:468-75.
36. Asadi S, Pirsa S. Production of biodegradable film based on polylactic acid, modified with lycopene pigment and TiO_2 and studying its

[DOI: 10.18502/jehsd.v10i1.18299]

physicochemical properties. J Polym Environ. 2020;28(2):433-44.
37. Jeun J-P, Jeon Y-K, Nho Y-C, et al. Effects of gamma irradiation on the thermal and mechanical properties of chitosan/PVA nanofibrous mats. Journal of Industrial and Engineering Chemistry. 2009;15(3):430-3.
38. Stuart BH. Infrared spectroscopy: fundamentals and applications. John Wiley & Sons; 2004.
39. Elsawy MA, Fekry M, Sayed AM, et al. Physico-chemical characteristics of biodegradable poly (lactic acid) and poly (lactic acid)/Chitosan nano-composites under the influence of gamma irradiation. J Polym Environ. 2023;31(6):2705-14.
40. Augustine R, Kalarikkal N, Thomas S. Effect of zinc oxide nanoparticles on the in vitro degradation of electrospun polycaprolactone membranes in simulated body fluid. International Journal of Polymeric Materials and Polymeric Biomaterials. 2016;65(1):28-37.

[DOI: 10.18502/jehsd.v10i1.18299]

